CHEMISTRY
A European Journal

A Journal of
ChemPubSoc Europe

Accepted Article

Title: Mapping the Assembly of Metal-organic Cages into Complex Coordination Networks

Authors: Ashok Yadav, Arvind Kumar Gupta, Alexander Steiner, and Ramamoorthy Boomishankar

To be cited as: *Chem. Eur. J.* 10.1002/chem.201704585

Link to VoR: http://dx.doi.org/10.1002/chem.201704585

Supported by
ACES

WILEY-VCH

10.1002/chem.201704585

WILEY-VCH

Mapping the Assembly of Metal-organic Cages into Complex Coordination Networks

Ashok Yadav,[a] Arvind K. Gupta,[a] Alexander Steiner*,[c] and Ramamoorthy Boomishankar*,[a,b]

Abstract: Structural transformations of supramolecular assemblies play an important role in the synthesis of complex metal-organic materials. Nonetheless, more than often little is known of the assembly pathways that lead to the final product. Herein, we describe the conversion of cubic metal-organic polyhedra to connected-cage networks of varying topologies. The neutral cubic cage assembly of formula $\{Pd_3[PO(N^iPr)_3]\}_8(PZDC)_{12}$ has been synthesized from $\{Pd_3[(N^iPr)_3PO](OAc)_2(OH)\}_2{\cdot}2(CH_3)_2SO$ and 2,5-pyrazenedicarboxilic acid (PZDC-2H). This 42-component self-assembly is the largest known among the neutral cages with Pd(II) ions. The cage contains twenty-four vacant carboxylate O-sites at the PZDC ligands that are available for further coordination. Post-assembly reactions of the cubic cage with Fe(II) and Zn(II) ions produced cage-connected networks of *dia* and *qtz* topologies, respectively. During these reactions, the discrete cubic cage transforms into a network of tetrahedral cages that are bridged by the 3d metal-ions. The robustness of the $[Pd_3\{[PO(N^iPr)_3\}]^{3+}$ molecular building units made it possible to map the post-assembly reactions in detail, which revealed a variety of intermediate 1D and 2D cage-networks. Such step-by-step mapping of the transformation of discrete cages to cage-connected frameworks is unprecedented in the chemistry of coordination driven assemblies.

Introduction

Structural rearrangements such as conversions, folding and association play an important role in biological reactions; well-known examples are microbial fission and fusion processes as well as enzyme catalysis.[1-3] Over the years, supramolecular self-assemblies in the form of grippers, capsules, cavitands, cages and polymers have been used to mimic such rearrangement processes that can be triggered by various external stimuli.[4-9] Several of the supramolecular rearrangement reactions follow assembly-disassembly-reassembly pathways wherein the overall structure of the original construct is maintained.[10-12] Such processes can also play an integral part in the construction of molecular devices.[13-20]

Metal-organic polyhedra (MOPs) or -cages (MOCs) built from the spontaneous assembly of smaller molecular constituents are an important class of compounds in supramolecular chemistry.[21-33] Multifunctional MOPs are highly desired for molecular recognition, biological activity, reactive species sequestration, catalysis and gas adsorption and separation.[34-43] Particularly interesting is the assembly of MOPs to generate hierarchical coordination networks. Utilizing metal-organic squares, cubes and octahedrons, cage-connected frameworks with varying dimensionalities and topologies have been obtained.[44-48] Similarly, cage-connected networks with 3D-topologies have been realized by employing carboxylate ligands and certain molecular-building units such as paddle-wheel motifs.[49-53]

The construction of MOPs and coordination networks usually involves many assembly and rearrangement steps. Normally, very little is known about the intermediates in these reactions. In some instances they could be studied by NMR, mass spectra and electron microscopy,[54-59] whereas obtaining X-ray structures of intermediates are often more challenging.[60,61] This can be attributed to the complex solution dynamics exhibited by the individual components of the MOPs as well as the unstable nature of the intermediates formed during such transformations.

Here, we describe the conversions of a cubic metal organic cage $[(Pd_3X)_8(PZDC)_{12}]$ (X = $[PO(N^iPr)_3]$) into 3D-frameworks of tetrahedral cages $[(Pd_3X)_4(PZDC)_6]$ that are linked via coordination of M(II) ions (M = Fe, Zn) to the vacant carboxylate oxygen sites of the PZDC ligand. The $[Pd_3X]^{3+}$ units have been shown to be very robust and versatile building blocks.[62-63] We were able to isolate and characterize intermediates that occur along the pathway to the 3D frameworks. These consisted of discrete cages and one- as well as two-dimensional cage-connected-frameworks. This enabled us to map the process of the conversion reactions and show that they proceed with sequential change of symmetries, which is a rare phenomenon in the chemistry of supramolecular cages.[64-67].

Results and Discussion

Treatment of $\{Pd_3X(OAc)_2(OH)\}_2{\cdot}2(CH_3)_2SO$ (**1**)[63], which contains tripodal $[Pd_3X]^{3+}$ units consisting of a triangular array of Pd(II) ions that is capped by the tripodal ligand $[PO(N^iPr)_3]^{3-}$ (= X^{3-}), with 2,5-pyrazenedicarboxilic acid (PZDC-2H) in a 1:3 ratio in MeOH/DMSO yielded a cubic cage assembly of composition $[(Pd_3X)_8(PZDC)_{12}]$, **2** (Scheme 1). The ^{31}P NMR of **2** recorded in DMSO gave a single peak at δ = 73.7 ppm characteristic of the tris-imido phosphate ligand. The MALDI-TOF spectrum showed a broad signal that is centered at the predicted molecular mass for this cage (m/z = 6730.23) (Figures S1-S2, Supporting Information).

[a] A.Yadav, Dr. A. K. Gupta and Prof. R. Boomishankar
Department of Chemistry, Indian Institute of Science Education and Research (IISER), Pune Dr. Homi Bhabha Road, Pune – 411008, India.
E-mail: boomi@iiserpune.ac.in
[b] Prof. R. Boomishankar
Centre for Energy Sciences, Indian Institute of Science Education and Research (IISER), Pune Dr. Homi Bhabha Road, Pune – 411008, India.
[c] Dr. A. Steiner
Department of Chemistry,
University of Liverpool,
Crown Street, Liverpool – L69 7ZD, United Kingdom.
E-mail: A.Steiner@liverpool.ac.uk

Electronic Supplementary Information (ESI) available: [CCDC 1573962-1573969 contains the supplementary crystallographic data. Additional figures and tables pertaining to crystal structures, NMR data]. See DOI: 10.1039/x0xx00000x

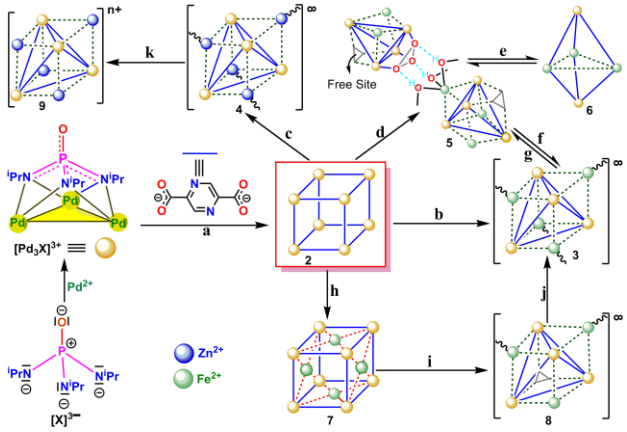

Scheme 1. Formation of the cubic assembly of **2** and the schematic representation of its post assembly reactions; the extra framework anions and solvate molecules have been omitted for clarity. Reaction conditions: (a) DMSO/MeOH at RT, (b) $Fe(OTf)_2$/MeOH at 70 °C, (c) $Zn(NO_3)_2$/MeOH at 25 °c. (d) $Fe(OTf)_2$/MeOH at 25 °c (e) slow evaporation of methanol (f) heating at 70 °C. Immersion of the crystals of 2 in Fe(OTf)2/MeOH (g) dilution by MeOH (h) for one month, (i) after two months and (j) after six months. (k) Suspending the polycrystalline sample of **4** in MeOH for 2 days.

The cubic assembly crystallizes in the form of the solvate **2**·6.5DMSO·22H_2O. The cubic cage comprises eight $[Pd_3X]^{3+}$ units (Figure 1a). Every Pd(II) ion is coordinated in a square planar fashion by a bidentate site of X^{3-} ligand and a bidentate N,O-site of bridging 2,5-pyrazenedicarboxylate anions (PZDC), while in return every PZDC ligand binds two Pd(II) ions in opposite N,O-sites (Figures 1b and 1c). The result is a cubic cage, in which the eight $[Pd_3X]^{3+}$ units occupy the vertices while the twelve PZDC ligands form its edges (Figure 1d and Figures S3-S5, Supporting Information). Altogether the cubic MOP assembly of **2** consists of 42 components. There are a few reports in literature that utilized PZDC ligands as linkers in coordination polymers.[68-70] However, the construction of MOFs/MOPs based on this ligand remained unexplored.

The presence of 24 non-coordinated carboxylate-O-atoms in **2** gave us the idea to populate those sites with metal ions. A summary of the post-assembly reactions showing the formation of the various networks and stable intermediates is shown in Scheme 1. Treatment of **2** with $Fe(OTf)_2$ in methanol under reflux conditions and subsequent storage of the solution gave yellowish-green crystals of **3**. Structural determination of **3** revealed the formation of a 3D cage-connected network of formula $[Fe_4(Pd_3X)_8(PZDC)_{12}(H_2O)_3](OTf)_8$·10DMSO·15$H_2O$ (Fig. 2a). The network comprises tetrahedral $[(Pd_3X)_4(PZDC)_6]$ cages, in which every Pd_3X unit coordinates three PZDC ligands and in return every PZDC ligand bridges between two Pd_3X units, which corresponds to the primary coordination pattern that was observed in **2**. These tetrahedral cages are fused via Fe(II) ions which occupy the tridentate coordination sites of three carboxylate-O-atoms located on each face of the tetrahedral cage (Figures 2c and 2d). As such, every $[(Pd_3X)_4(PZDC)_6]$ cage acts as a tetrahedral 4-connector resulting in a net with a diamond-type topology (*dia* net, Figures 2e and S6-S7, Supporting Information).[71-72] The rhombohedral cell (*R*3) contains two crystallographically unique cages and eight unique Fe(II) ions, two of which are octahedrally coordinated by two tridentate cage sites, while the remaining six ions display an unusual seven-coordinated environment consisting of two tridentate cage sites and one water ligand.

The reaction of **2** with $Zn(NO_3)_2$·6H_2O in methanol at room temperature yielded yellowish-orange crystals, which again consists of a 3D-network that feature tetrahedral $[(Pd_3X)_4(PZDC)_6]$ cages that are networked via Zn(II) ions (Figure 2b). The crystals of **4** ($P3_121$) are of composition $[Zn_2(Pd_3X)_4(PZDC)_6(H_2O)_4](NO_3)_4$·16$H_2O$. In contrast to the Fe(II) derivative **3**, they exhibit a chiral network of quartz-type topology (*qtz* net, Figures 2f, and S8-S11, Supporting Information). It is noteworthy that the coordination sphere of Zn ions is even more expanded exhibiting an 8-coordinate square antiprismatic environment of four carboxylate-O-sites and two water molecules.

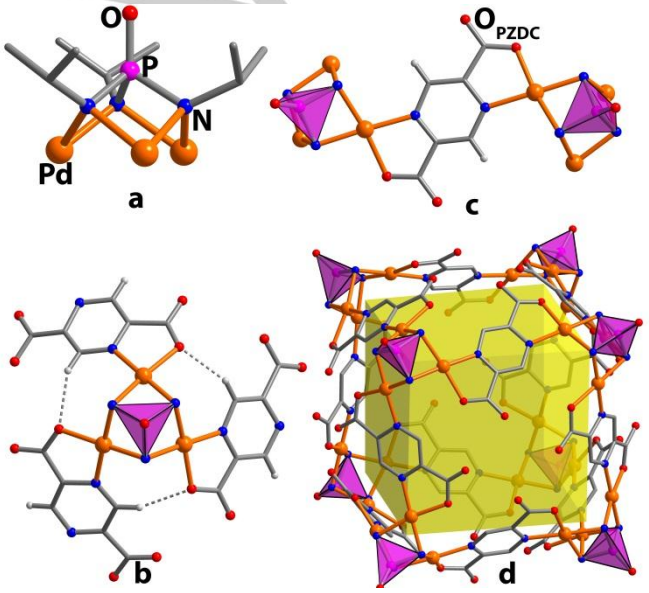

Figure 1. Crystal structure of **2**. (a-c) Schematic view of the $[Pd_3X]^{3+}$ PBU and its coordination with the PZDC anions leading to the formation of the 42-component cubic cage (d). PON_3 units shown as purple tetrahedra in b-d.

In both **3** and **4,** the basic structural motif is the heterobimetallic cubane of the type $[M_4(Pd_3X)_4(PZDC)_6]$ in which the Pd_3X-PBUs form primary tetrahedral nodes that are connected via Fe(II) and Zn(II) ions. However, the increased coordination spheres around these ions indicate a deviation of linearity of the cage-M-cage axes. The cage(centroid)-M-cage(centroid) angles are 180° for the 6-coordinate Fe(II) and 146° for the 7-coordinate Fe(II) ion in **3**, while it is 145° in **4**. This angle seems to provide for a closer packing of cages; in addition to metal coordination, it also enables Van-der-Waals interactions between the cages. In return, the deviation from linearity between cages exposes the M(II) ions and thereby expanding the coordination sphere leading to hyper-coordination (Figures S12-S13, Supporting Information).

10.1002/chem.201704585

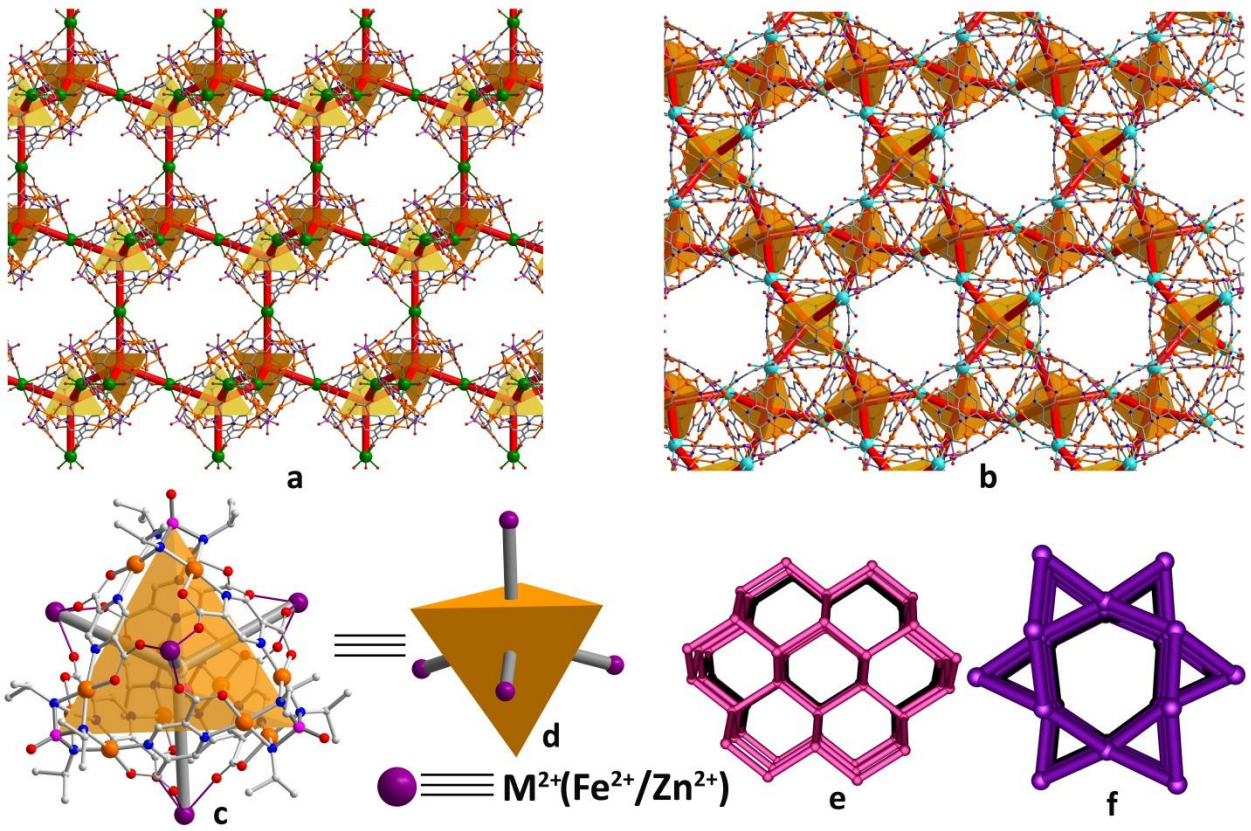

Figure 2. Crystal Structures of **3** (a) and **4** (b). (c) View of a single isostructural tetrahedral cage of **3** and **4**. (d) Simplified 4-connected representation of the tetrahedral cage; (e) and (f) show the network structures of **3** (*dia* net) and **4** (*qtz* net), respectively. Green and cyan coloured spheres represent Fe (II) and Zn (II) atoms.

To understand the formation of these cage-connected 3D-assemblies, we repeated the reactions under milder conditions. The treatment of **2** with $Fe(OTf)_2$ in MeOH at 25 °C resulted in a spontaneous colour change from orange to green. Dark green coloured crystals of **5** of composition $[Fe_7(Pd_3X)_{12}(PZDC)_{18}(CH_3OH)_7(H_2O)_7](OTf)_{14}\cdot 8H_2O$, were recovered from this solution (Figures S14-S18, Supporting Information). As for **3**, this compound also consists of $[(Pd_3X)_4(PZDC)_6]$ cages. However, in contrast to **3**, not all of the four tridentate carboxylate-O-sites are occupied by connecting Fe(II) ions. There are two crystallographically unique cages present in a 2:1 ratio; these are depicted orange and blue in Figure 3. All four tridentate sites of the 'blue' cage form bridges to neighbouring cages. These bridges consist of an arrangement where one tridentate site accommodates a metal ion, while the opposite site at the other cage forms hydrogen bonds to the methanol/water ligands coordinated to the metal ion that belongs to the first cage. Figure 3a shows this arrangement of metal-coordination/hydrogen-bonding linkage. The 'orange' cage, meanwhile, forms three of these bridges while the fourth site is occupied by a terminal, non-bridging Fe(II) ion. Hence, the 'blue' cages act as tetrahedral 4-connectors, while the 'orange' cages are trigonal pyramidal 3-connectors. The resulting network is a puckered 2D-grid with pentagonal rings (Figure 3b).

When the green crystals of **5** were dissolved and the solution was heated at 70 °C for 4 h, the green solution turns yellow and yellowish green crystals of **3** were again obtained after 3-4 days (Figure S19, Supporting Information). It is easy to imagine that elimination of the three methanol ligands from the metal-coordination/hydrogen-bonding-bridge generates the more direct all metal-coordination mode between the two cages that is observed in **3** (and in **8**, Figure 6). Hence, **5** can be regarded as a kind of intermediate along the pathway toward the coordination network of **3** (Figure 3c).

Concentrating the green coloured solution of **5** by half of its original volume and leaving it standing gave blue crystals. The structural determination of these crystals revealed the formation of a compound of formula $[Fe_3(Pd_3X)_2(PZDC)_6(H_2O)_6]\cdot 2CH_3OH\cdot 2DMSO\cdot 22H_2O$ (**6**) (Figure 4 and S20-S24, Supporting Information). This structure consists of trigonal bipyramidal $[Fe_3(Pd_3X)_2(PZDC)_6]$ cages where the Fe ions occupy the equatorial and the Pd_3X units at the axial sites.

In contrast to the cubic and tetrahedral cages of **2** and **3**, the PZDC ligands in **6** do not act as a bridge between two Pd_3X components. Instead, it can be regarded as an assembly containing two separate $[Pd_3X(PZDC)_3]^{3-}$ entities that are linked by Fe(II) ions (Figure 4). The coordination geometry around the Fe(II) ions can be described as distorted octahedral consisting of the O-sites of four PZDC ligands and two water molecules which are in mutual cis-position (Figure S25, Supporting Information).

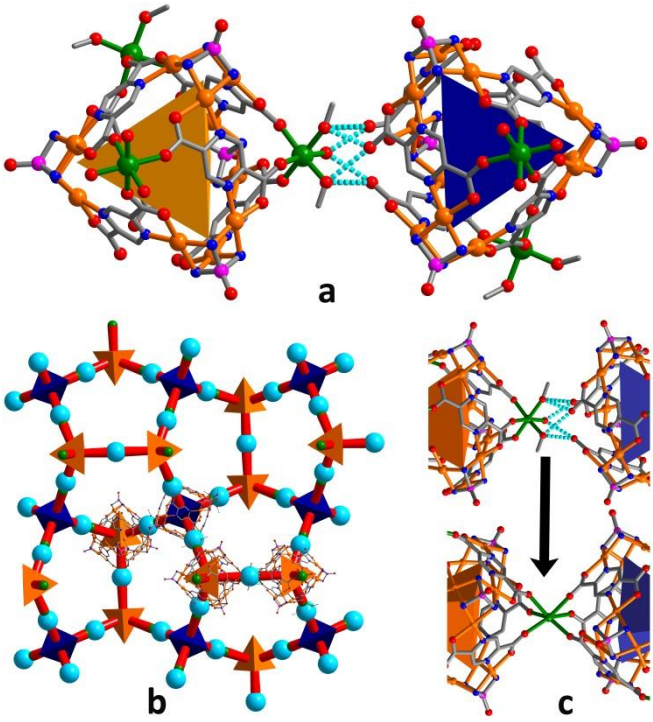

Figure 3. (a) Crystal structure of **5** highlighting the metal coordination/hydrogen bonding bridge (H-bonds drawn as dashed lines). (b) The puckered layered network in **5** (metal coordination/hydrogen bonding bridges are shown as cyan spheres). (c) Metal coordination/hydrogen bonding bridge can be regarded as precursor to direct metal coordination link (observed as in **3** and **8**).

The conversion of the tetrahedral (in **3**) to the trigonal bipyramidal cage can also be observed in solution. Repeated concentration by solvent evaporation and subsequent replenishment with methanol leads to colour changes to and from green (**5**) to blue (**6**) (Figure 5a). Upon heating the green colored solution of **5**, the tetrahedra condense to form the 3D-assembly of **3**. The ^{31}P- and ^{1}H-NMR spectra recorded on the reaction mixture of **2** and $Fe(OTf)_2$ in CD_3OD after 24 h gave the signals corresponding to both **5** and **6** (Figures 5b and S26-S27, Supporting Information). These observations were further supported by the ^{1}H-2D-DOSY NMR spectrum of the reaction mixture which gave two diffusion coefficients (D) at 8.25×10^{-11} and 8.31×10^{-10} m^2s^{-1} indicating the presence of **5** and **6**, respectively (Figures S28-S30, Supporting Information). The MALDI-TOF mass spectra of the reaction mixture recorded at different intervals show a progressive change of intensities for the peaks due to **5** and **6** (Figures 5c-f). The ^{31}P-NMR of a sample of **3** to which methanol was added gave peaks due to both **5** and **6**. These peaks suggest equilibria in solution between the heterometallic assemblies of **3**, **5** and **6**. There are some reports on structural inter-conversions of discrete cage-assemblies in the recent literature.[73]

In order to stop the process of conversion at an even earlier stage, we carefully covered the crystals of **2** with a solution of $Fe(OTf)_2$ in methanol. After one month the crystals showed a visible change in colour from orange to dark yellow. Structural analysis showed the formation of a heterobimetallic cage assembly **7** of composition $[Fe_2(Pd_3X)_8(PZDC)_{12}(H_2O)_8](OTf)_8\cdot8DMSO\cdot59H_2O$, which features the same cubic cage structure $[(Pd_3X)_8(PZDC)_{12}]$ as observed in **2** (Figures 6a and S31, Supporting Information). In contrast to the tetrahedral cage $[(Pd_3X)_4(PZDC)_6]$ (as in **3** and **4**), which offers four tridentate carboxylate-O-sites, the cubic cage $[(Pd_3X)_8(PZDC)_{12}]$ provides six tetradentate carboxylate-O-sites of square planar geometry. In **7** four of these sites are occupied by Fe(II) ions. Compared to the non-coordinated cage of **2**, the cage in **7** shows a slight tetragonal distortion, when measured between the centroids of the four carboxylate-O-atoms of the tetradentate coordination site centers. The distance between opposite sites coordinated by Fe(II) ions is 14.8 Å, whereas it is 15.3 Å between the two non-coordinated sites.

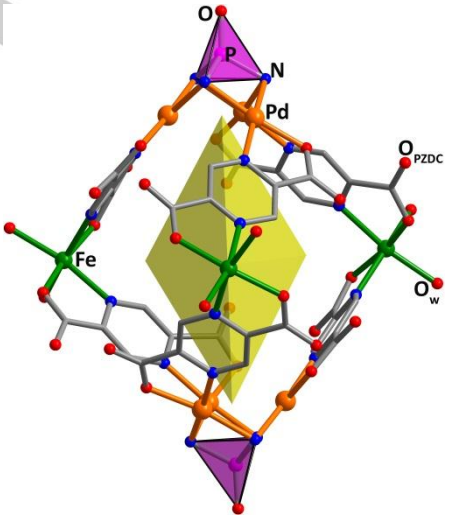

Figure 4. Crystal Structure of **6**.

The colour of the crystals changed to light-yellow after two-months. These consist of tetrahedral cages that are connected via Fe(II) ions into a helical chain (Figure 6b). The other two tridentate sites of the cages are partially occupied by Fe(II) ions exhibiting occupancy factors of roughly ½ and ¼, respectively, and do not form linkages to other cages. The overall composition of **8** is $[Fe_{1.75}(Pd_3X)_4(PZDC)_6(H_2O)_{3.5}]\cdot(OTf)_{3.5}\cdot24H_2O$. The bridging Fe(II) ions have distorted octahedral geometry (Figure 6b and S32, Supporting Information). The pitch of the helical chain

contains four cages; its length is 28.6 Å and its width 30.8 Å. Again, the cage(centroid)-Fe-cage(centroid) angles deviate from linearity; they measure 162 and 176°, respectively. It is noteworthy that such helical chains can also be found as segments in the 3D-network of **3**. Eventually, after six months of storage the diamondoid framework of **3** was formed again (Figure S33, Supporting Information).

Similar attempts to trace potential intermediates in the Zn-system remained futile. However, when a suspension of a polycrystalline sample of **4** in methanol was left for crystallization, it gave rise to $[Zn_3(Pd_3X)_4(PZDC)_6(H_2O)_9](NO_3)_6{\cdot}2DMSO{\cdot}6H_2O$, **9**. It also contains tetrahedral cages and all four tridentate sites are accommodated by Zn(II) ions, albeit with somewhat reduced occupancies (Figure 6c). The cages are not part of coordination network and can be regarded as more or less a discrete assembly with a zeolitic D4R topology (Figure S34, Supporting Information).[74]

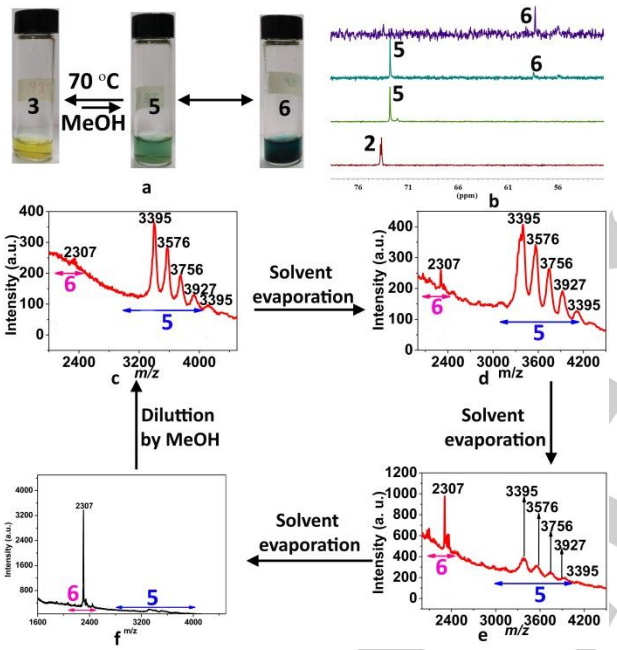

Figure 5. (a) Solution color changes involved in the structural transformations. (b) ^{31}P NMR spectra of the reaction mixture of **2** and $Fe(OTf)_2$ showing the formation of **5** and **6** at various intervals. (c)-(f) MALDI-TOF mass spectra of the reaction mixture of **2** with $Fe(OTf)_2$ taken at various intervals showing the gradual conversion of **5** to **6**; (c) after one day, (d) after three days, (e) after six days and (f) after 8 days**.** Upon dilution in methanol **6** is converted back to **5** in 1h by a structural rearrangement.

However, as shown above, fine-tuning of the reaction conditions of the Fe(II)-system allowed us to trap the various stages of the conversions. Treating the system at elevated temperature in solution ultimately yields the 3D-network, whereas careful submersion of precursor crystals in the solvent enabled the isolation of intermediates. The presence of crystals thoughout this process may suggest direct single-crystal-to-single-crystal transformations. However, the accompanying changes to the crystal structures may be too substantial to maintain the integrity of the single crystal. More likely these conversions occur via mass-transport by slow diffusion.[75]

The results suggest that the post-assembly conversion of the cubic cage (**2**) is first initiated by stepwise accommodation of Fe(II) ions into the tetradentate sites of the cubic cage (**7**) (Scheme 2). The next step involves re-arrangement from a cubic to a tetrahedral cage, which is most likely to be triggered by M(II) coordination. A comparison of the crystal structures of **2** and **7** reveals that the coordination of the Fe(II) ions at the cube-faces leads to tetragonal distortions which may trigger the cleavage of the cubic assembly. Although the stoichiometry of tetrahedral and cubic cages are equivalent ($[(Pd_3X)_4(PZDC)_6]$ vs. $[(Pd_3X)_8(PZDC)_{12}]$), which may suggest that simple fission of the cubic cages generates two tetrahedral cages, it remains impossible to formulate a definite mechanism for this re-arrangement from our current data.

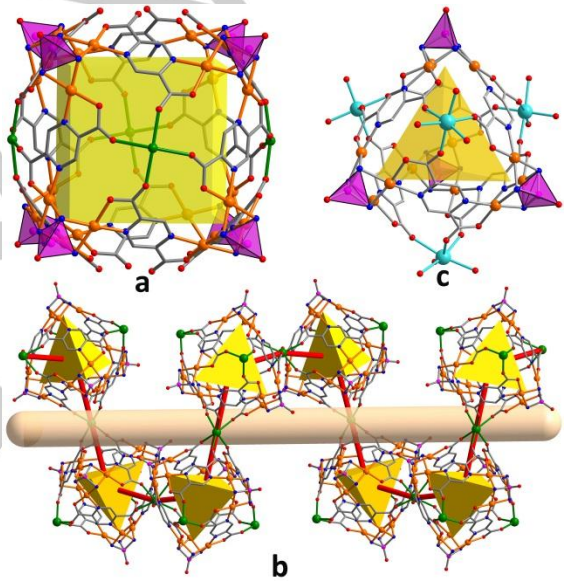

Figure 6. (a) Crystal structure of **7**. (b) Helical chain structure of **6.** (c) Molecular structure of **9**.

Structural comparison between the two cages (cubic and tetrahedral) shows that the primary coordination of Pd_3X and PZDC components is the same for both cages. However, the radius of the canopy that is formed by the arrangement of a Pd_3X unit and its three surrounding PZDC ligands is smaller for the tetrahedral cage (5.5 Å) than for the cubic cage (6.5 Å), which indicates that this arrangement is flexible and therefore able to adapt to various cage geometries. This is also evident from the formation of the trigonal bipyramidal assembly of **6**, which shows the competition of Pd(II) and Fe(II) ions for the coordination with the PZDC ligands.

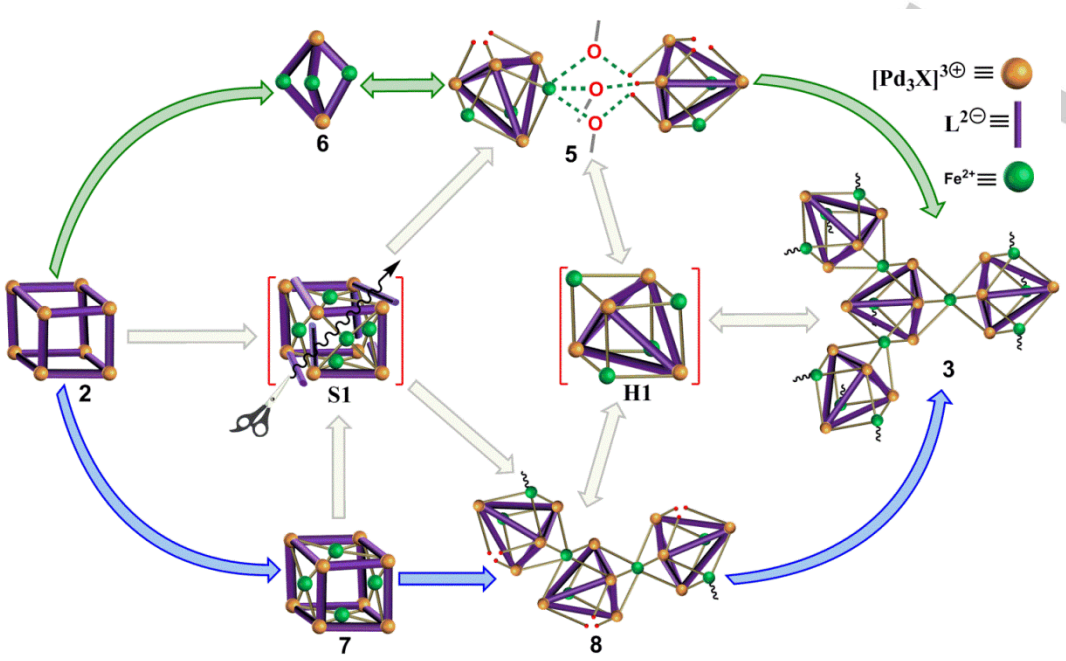

Scheme 2. Summary of the step-wise post-assembly reactions involving **2** and Fe^{2+} ions; green arrows indicate conversions of fully dissolved samples wheras the blue arrows denote conversions that occur via slow diffusion between crystals. **S1**, **H1** and the grey arrows are shown to illustrate the relationship between the isolated cage compounds. **S1** represents the cleavage of cubic to tetrahedral cages. **H1** emphasizes the shared heterometallic tetrahedral cage of **3**, **5** and **8**.

The pathway of linking the cages can be envisaged via the metal-coordination/hydrogen bonding bridge as observed in **5**. Simple elimination of the three metal-coordinated solvent molecules accomplishes the direct coordination mode, where both cages bind to the metal ion. Consequently, this will lead to coordination networks of increasing connectivity. The networks with the highest connectivity (**3** and **4**) seem to be the thermodynamically favoured products for both Fe(II) and Zn(II) bridged systems. The choice of metal ion seems to influence the topology of the resulting net. It appears that this is governed by a fine balance between maximising the cage interactions and the coordination requirements of the metal ion. Also, the conversion of the cubic cage to the tetrahedral frameworks involves a series of lower symmetric intermediates. It is interesting to note that parallels of these cage conversions that involve polyhedra of different symmetries to developmental biology, where symmetry breaking can be correlated to cellular differentiation in which genome speciation of Zygote leads to a system of complex tissues.[76-78]

Conclusions

In summary, we have utilized a neutral cubic cage with active coordinating groups for assembling cc-MOFs with *dia* and *qtz* topologies. The neutral cubic cage **2** was obtained in a 42-component self-assembly reaction and is the largest for the neutral homoleptic cage assemblies known for Pd(II) ions. The post-assembly reaction of **2** with $Fe(OTf)_2$ could be performed in a controlled fashion giving rise to a series of hierarchical heterobimetallic assemblies of discrete, 1D and 2D-architectures, which can be regarded as intermediate stages along the pathway to the final 3D-framework. The topology of the final 3D-framework is governed by the choice of 3d metal-ion; Fe(II) generates a *dia*, Zn(II) a *qtz* net. Mapping the pathways of the conversion reactions revealed that these proceed with sequential change of cage-symmetries. It shows that the stepwise transformation of the discrete cubic cage to the networks of tetrahedral cages is triggered and controlled by the coordination of the 3d metal ions. Such sequential symmetry conversions are rare in metal-organic self-assemblies. They could pave the way for new design strategies towards complex coordination networks and framework structures.

Acknowledgements

This work was supported by SERB, India through Grant No. EMR/2016/000614 (R.B.). A.Y. thanks the Council of Scientific and Industrial Research for the fellowship.

Keywords: metal-organic polyhedra • cage-framework • topology • inter-conversion

References

[1] K. A. Dill, J. L. MacCallum, *Science* **2012**, *338*, 1042-1046.
[2] B. Pearse, *Proc. Nat. Acad. Sci.* **1976**, *73*, 1255-1259.
[3] S. M. Stagg, P. LaPointe, A.; Razvi, C. Gürkan, C. S. Potter, B. Carragher, W. E. Balch, *Cell* **2008**, *134*, 474-484.
[4] M. Han, D. M. Engelhard, G. H. Clever, *Chem. Soc. Rev.* **2014**, *43*, 1848-1860.
[5] Y. Hua, Y. Liu, C. H. Chen, A. H. Flood, *J. Am. Chem. Soc.* **2013**, *135*, 14401-14412.
[6] J. Mosquera, T. K. Ronson, J. R. Nitschke, *J. Am. Chem. Soc.* **2016**, *138*, 1812-1815.
[7] Y. Murakami, O. Hayashida, *Proc. Nat. Acad. Sci.* **1993**, *90*, 1140-1145.
[8] I. Pochorovski, M. O. Ebert, J. P. Gisselbrecht, C. Boudon, W. B. Schweizer, F. Diederich, *J. Am. Chem. Soc.* **2012**, *134*, 14702-14705.
[9] D. Samanta, P. S. Mukherjee, *Chem. Eur. J.* **2014**, *20*, 12483-12492.
[10] M. E. Carnes, M. S. Collins, D. W. Johnson, *Chem. Soc. Rev.* **2014**, *43*, 1825-1834.
[11] M. Fujita, O. Sasaki, T. Mitsuhashi, T. Fujita, J. Yazaki, K. Yamaguchi, K. Ogura, *Chem. Commun.* **1996**, 1535-1536.
[12] M. Schweiger, S. R. Seidel, A. M. Arif, P. J. Stang, *Inorg. Chem.* **2002**, *41*, 2556-2559.
[13] V. Balzani, A. Credi, F. M. Raymo, J. F. Stoddart, *Angew. Chem. Int. Ed.*, **2000**, *39*, 3348-3391.
[14] V. Balzani, A. Credi, M. Venturi, *Proc. Nat. Acad. Sci. U.S.A.* **2002**, *99*, 4814-4817.
[15] V. Balzani, M. Gómez-López, J. F. Stoddart, *Acc. Chem. Res.* **1998**, *31*, 405-414.
[16] V. Balzani, F. Scandola, Supramolecular Photochemistry (Horwood, Chichester, U.K.), **2000**.
[17] P. Barbara, J. F. Stoddard, J. *Acc. Chem. Res.* **2001**, *34*, 409.
[18] A. P. De Silva, H. N. Gunaratne, T. Gunnlaugsson, A. J. Huxley, C. P. McCoy, J. T. Rademacher, T. E. Rice, *Chem. Rev.* **1997**, *97*, 1515-1566.
[19] J. M. Lehn, *Angew. Chem. Int. Ed.* **1988**, *27*, 89-112.
[20] J. M. Tour, *Acc. Chem. Res.*, **2000**, *33*, 791-804.
[21] D. L. Caulder, C. Brückner, R. E. Powers, S. König, T. N. Parac, J. A. Leary, K. N. Raymond, *J. Am. Chem.Soc.* **2001**, *123*, 8923-8938.
[22] R. Chakrabarty, P. S. Mukherjee, P. J. Stang, *Chem. Rev.* **2011**, *111*, 6810-6918.
[23] E. C. Constable, G. Zhang, D. Häussinger, C. E. Housecroft, J. A. Zampese, *J. Am. Chem. Soc.* **2011**, *133*, 10776-10779.
[24] T. R. Cook, Y. R. Zheng, P. J. Stang, *Chem. Rev.*, **2012**, *113*, 734-777.
[25] J. H. Fu, Y. H. Lee, Y. J. He, Y. T. Chan, *Angew. Chem. Int. Ed.* **2015**, *54*, 6231-6235.
[26] M. Han, Y. Luo, B. Damaschke, L. Gómez, X. Ribas, A. Jose, P. Peretzki, M. Seibt and G. H. Clever, *Angew. Chem. Int. Ed.*, **2016**, *55*, 445-449.
[27] K. Harris, D. Fujita, M. Fujita, *Chem. Commun.* **2013**, *49*, 6703-6712.
[28] T. Kusukawa, M. Fujita, *J. Am. Chem. Soc.* **2002**, *124*, 13576-13582.
[29] A. J. McConnell, C. S. Wood, P. P. Neelakandan, J. R. Nitschke, *Chem. Rev.*, **2015**, *115*, 7729-7793.
[30] B. Olenyuk, M. D. Levin, J. A. Whiteford, J. E. Shield, P. J. Stang, *J. Am. Chem. Soc.*, **1999**, *121*, 10434-10435.
[31] Q. F. Sun, J. Iwasa, D. Ogawa, Y. Ishido, S. Sato, T. Ozeki, Y. Sei, K. Yamaguchi, M. Fujita, *Science* **2010**, *328*, 1144-1147.
[32] M. Wang, K. Wang, C. Wang, M. Huang, X. Q. Hao, M. Z. Shen, G. Q. Shi, Z. Zhang, B. Song, A. Cisneros, *J. Am. Chem. Soc.* **2016**, *138*, 9258-9268.
[33] W. Wang, Y. X. Wang, H. B. Yang, *Chem. Soc. Rev.* **2016**, *45*, 2656-2693.
[34] D. Ajami, J. Rebek, *Proc. Nat. Acad. Sci.* **2007**, *104*, 16000-16003.
[35] C. J. Brown, F. D. Toste, R. G. Bergman, K. N. Raymond, *Chem. Rev.* **2015**, *115*, 3012-3035.
[36] T. R. Cook, V. Vajpayee, M. H. Lee, P. J. Stang, K. W. Chi, *Acc. Chem. Res.* **2013**, *46*, 2464-2474.
[37] R. Custelcean, P. V. Bonnesen, N. C. Duncan, X. Zhang, L. A. Watson, G. Van Berkel, W. B. Parson, B. P. Hay, *J. Am. Chem. Soc.* **2012**, *134*, 8525-8534.
[38] R. A. Kaner, P. Scott, *Future med. Chem.* **2015**, *7*, 1-4.
[39] S. H. Leenders, R. Gramage-Doria, B. de Bruin, J. N. Reek, *Chem. Soc. Rev.* **2015**, *44*, 433-448.
[40] A. M. Lifschitz, M. S. Rosen, C. M. McGuirk, C. A. Mirkin, *J. Am. Chem. Soc.*, **2015**, *137*, 7252-7261.
[41] P. Mal, B. Breiner, K. Rissanen, J. R. Nitschke, *Science*, **2009**, *324*, 1697-1699.
[42] M. J. Wiester, P. A. Ulmann, C. A. Mirkin, *Angew. Chem. Int. Ed.* **2011**, *50*, 114-137.
[43] M. Yamashina, Y. Sei, M. Akita, M. Yoshizawa, *Nat. Commun.* **2014**, *5*.
[44] S. Wang, T. Zhao, G. Li, L. Wojtas, Q. Huo, M. Eddaoudi, Y. Liu, *J. Am. Chem. Soc.* **2010**, *132*, 18038-18041
[45] Y. Liu, V. Kravtsov, R. D. Walsh, P. Poddar, H. Srikanth, M. Eddaoudi, *Chem. Commun.* **2004**, 2806-2807
[46] R.-Q. Zou, H. Sakurai, Q. Xu, *Angew. Chem. Int. Ed.* **2006**, *45*, 2542-2546.
[47] D. Moon, S. Kang, J. Park, K. Lee, R. P. John, H. G. Won, H. Seong, Y. S. Kim, G. Kim, H. H. Rhee, M. S. Lah, *J. Am. Chem. Soc.* **2006**, *128*, 3530-3531.
[48] A. J. Cairns, J. A. Perman, L. Wojtas, V. Ch. Kravtsov, M. H. Alkordi, M. Eddaoudi, M. J. Zaworotko, *J. Am. Chem. Soc.* **2008**, *130*, 1560-1561.
[49] R. V. Parish, Z. Salehi, R. G. Pritchard, *Angew. Chem. Int. Ed.* **1997**, *36*, 251-253.
[50] J. J. Perry, V. Ch. Kravtsov, G. J. McManus, M. J. Zaworotko, *J. Am. Chem. Soc.* **2007**, *129*, 10076-10077.
[51] F. Nouar, J. F. Eubank , T. Bousquet, L. Wojtas, M. J. Zaworotko and M. Eddaoudi, *J. Am. Chem. Soc.*, **2008**, *130*, 1833-1835.
[52] Z. Wang, V. Ch. Kravtsov, M. J. Zaworotko, *Angew. Chem. Int. Ed.* **2005**, *44*, 2877-2880.
[53] D. Li, T. Wu, X.-P. Zhou, R. Zhou, X.-C. Huang, *Angew. Chem. Int. Ed.* **2005**, *44*, 4175-4178.
[54] B. Kilbas, S. Mirtschin, R. Scopelliti, K. Severin, *Chem. Sci.* **2012**, *3*, 701-704.
[55] N. Kishi, M. Akita, M. Yoshizawa, *Angew. Chem. Int. Ed.* **2014**, *53*, 3604-3607.
[56] X. Lu, X. Li, K. Guo, T. Z. Xie, C. N. Moorefield, C. Wesdemiotis, G. R. Newkome, *J. Am. Chem. Soc.* **2014**, *136*, 18149-18155.
[57] W. Wang, Y. X. Wang, H. B. Yang, *Chem. Soc. Rev.* **2016**, *45*, 2656-2693.
[58] T. Z. Xie, K. Guo, Z. Guo, W. Y. Gao, L. Wojtas, G. H. Ning, M. Huang, X. Lu, J. Y. Li, S. Y. Liao, *Angew. Chem.* **2015**, *127*, 9356-9361.
[59] T.-Z. Xie, K. J. Endres, Z. Guo, J. M. Ludlow III, C. N. Moorefield, M. J. Saunders, C. Wesdemiotis, G. R. Newkome, *J. Am. Chem. Soc.* **2016**, *138*, 12344-12347.
[60] X.–P. Zhou, Y. Wu, D. Li, *J. Am. Chem. Soc.* **2016**, *135*, 16062-16065.
[61] W. Cullen, C. A. Hunter, M. D. Ward, *Inorg. Chem.* **2015**, *54*, 2626-2637.
[62] A. K. Gupta, A. Yadav, A. K. Srivastava, K. R. Ramya, H. Paithankar, S. Nandi, J. Chugh, R. Boomishankar, *Inorg. Chem.* **2015**, *54*, 3196-3202.
[63] A. K. Gupta, S. A. D. Reddy, R. Boomishankar, *Inorg. Chem.* **2013**, *52*, 7608-7614.
[64] W. Meng, T. K. Ronson, J. R. Nitschke, *Proc. Nat. Acad. Sci.* **2013**, *110*, 10531-10535.
[65] C. Olivier, E. Solari, R. Scopelliti, K. Severin, *Inorg. Chem.* **2008**, *47*, 4454-4456.
[66] R. W. Saalfrank, H. Maid, A. Scheurer, F. W. Heinemann, R. Puchta, W. Bauer, D. Stern, D. Stalke, *Angew. Chem. Int. Ed.* **2008**, *47*, 8941-8945.
[67] Y. Li, W. B. Zhang, I.-F. Hsieh, G. Zhang, Y. Cao, X. Li, C. Wesdemiotis, B. Lotz, H. Xiong, S. Z. Cheng, *J. .Am. Chem. Soc.* **2011**, *133*, 10712-10715.

[68] G. Beobide, O. Castillo, A. Luque, U. García-Couceiro, J. P. García-Terán, P. Román, *Inorg. Chem.* **2006**, *45*, 5367-5382.
[69] B. Cai, P. Yang, J. W. Dai, J. Z. Wu, *Cryst. Eng. Comm.* **2011**, *13*, 985-991.
[70] Y. Pan, D. Ma, H. Liu, H. Wu, D. He, Y. Li, *J. Mater. Chem.* **2012**, *22*, 10834-10839.
[71] M. O'Keeffe, O. M. Yaghi, *Chem. Rev.* **2011**, *112*, 675-702.
[72] E. V. Alexandrov, V. A. Blatov, A. V. Kochetkov, D. M. Proserpio, *Cryst.Eng.Comm.* **2011**, *13*, 3947-3958.
[73] W. Wang, Y.-X. Wang, H.-B. Yang, *Chem. Soc. Rev.* **2016**, *45*, 2656-2693.
[74] R. Murugavel, S. Kuppuswamy, R. Boomishankar, A. Steiner, *Angew. Chem. Int .Ed.* **2006**, *45*, 5536-5540.
[75] P. I. Richards, J. F. Bickley, R. Boomishankar, A. Steiner, *Chem. Commun.* **2008**, 1656-1658.
[76] R. Li, B. Bowerman, *Cold Spring Harb. Perspect. Biol.* **2010**, *2*, a003475.
[77] R. D. Mullins, *Cold Spring Harb. Perspect. Biol.* **2010**, *2*, a003392.
[78] J. M. W. Slack, *Nat. Rev. Mol. Cell Biol.* **2007**, *8*, 369-378.

10.1002/chem.201704585

WILEY-VCH

Entry for the Table of Contents

FULL PAPER

Fusion of cubes: Conversion of a cubic metal-organic polyhedron to connected-cage 3D-networks of varying topologies is reported. Structural chracterization of various 1D- and 2D-intermediate assemblies unfolds a fully mapped pathway for these conversions.

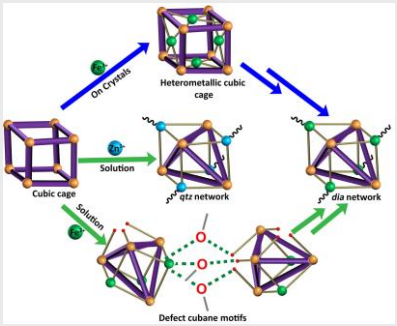

Ashok Yadav, Arvind K. Gupta, Alexander Steiner, and Ramamoorthy Boomishankar**

Page No. – Page No.

Mapping the Assembly of Metal-organic Cages into Complex Coordination Networks